1

Carbonation and Induced Steel Corrosion

This chapter treats the first important durability process of concrete materials and structures: the carbonation and the induced corrosion of steel bars in concrete. The carbonation of concrete originates from the reaction between the alkaline pore solution of concrete and the carbon dioxide (CO_2) gas migrating into the pores. The carbonation does not compromise the material properties but decreases the alkalinity of the pore solution, which has an adverse effect on the electrochemical stability of steel bars in concrete. The risk of steel corrosion can be substantially enhanced in a carbonated concrete. This chapter begins with the phenomena of concrete carbonation and its effect on the long-term durability of concrete materials and structures. Then the detailed mechanisms are presented, according to the state of the art of knowledge, for concrete carbonation and the induced steel corrosion, together with a comprehensive analysis on the main influential factors for these processes. On the basis of the available knowledge, the modeling aspect is brought forth through mechanism-based and empirical models for engineering use. Since the valid scope and the uncertainty are two fundamental aspects for model application, the critical analysis is given to the models presented and their application. Some basis for durability design against the carbonation and the induced corrosion is given at the end.

1.1 Phenomena and Observations

As concrete is exposed to the atmosphere, the CO_2 present in the atmosphere can migrate into the material through the pore structure and react with the cement hydrates such as portlandite ($Ca(OH)_2$ or CH) and the calcium silicate hydrates (C-S-H). These reactions are termed the "carbonation" of concrete materials. The direct consequence of carbonation is the consumption of CH, eventually C-S-H, and the decrease in pH value of the pore solution. Under a less alkaline environment, the electrochemical stability of the embedded steel bars in concrete can be destroyed, the steel can be depassivated and the electrochemical process of corrosion can

Durability Design of Concrete Structures: Phenomena, Modeling, and Practice, First Edition. Kefei Li.

Figure 1.1 Rebar corrosion of RC slabs in a fine-art gallery of age 38 years by concrete carbonation. The building was constructed in 1962 with C25 concrete for the RC beams. The concrete binder is ordinary Portland cement (OPC), and the building was exposed to a rather dry environment with average temperature of 11 °C and average humidity of 57%. *Source:* courtesy of Tianshen Zhang.

occur. As the corrosion develops to a significant extent, the reaction products from corrosion accumulate at the concrete–steel interface and can fracture the concrete cover. Since all concrete structures are built and used in the envelope of the atmosphere, carbonation is a basic and fundamental process for the long-term durability of concrete elements. Note that the detrimental aspect of carbonation resides mainly in the corrosion risk for the embedded steel bars and the carbonation itself is not found detrimental to concrete materials. Relevant studies show that the products of the carbonation reaction can notably reduce the porosity of hardened concrete, and the carbonation can also be used as a pretreatment technique for the recycled coarse aggregates to reduce the water sorptivity (Thiery *et al.*, 2013).

Concrete carbonation has been well investigated with regard to both the reaction mechanism and the alteration of properties of material and structural elements. The mechanism of carbonation is to be detailed later, while the most severe deterioration of concrete elements by carbonation is usually due to the less compacted concrete, insufficient protection of steel bars from the concrete cover, and the favorable moisture conditions for steel corrosion. For residential buildings, most reinforced concrete (RC) elements, like slabs and walls, usually bear surface lining or protection layers; thus, relatively few severe deterioration cases are reported for these elements by carbonation until a very late stage of service life. Nevertheless, the RC elements exposed directly to atmospheric precipitation, such as roofs, can show very advanced deterioration due to carbonation. Figure 1.1 illustrates an advanced state of carbonation-induced corrosion of reinforced steel bars of RC slabs in a fine-art gallery of age 38 years.

Compared with residential buildings, certain industrial buildings contain more aggressive environments for the concrete elements; for example, the concrete roofs of steel process

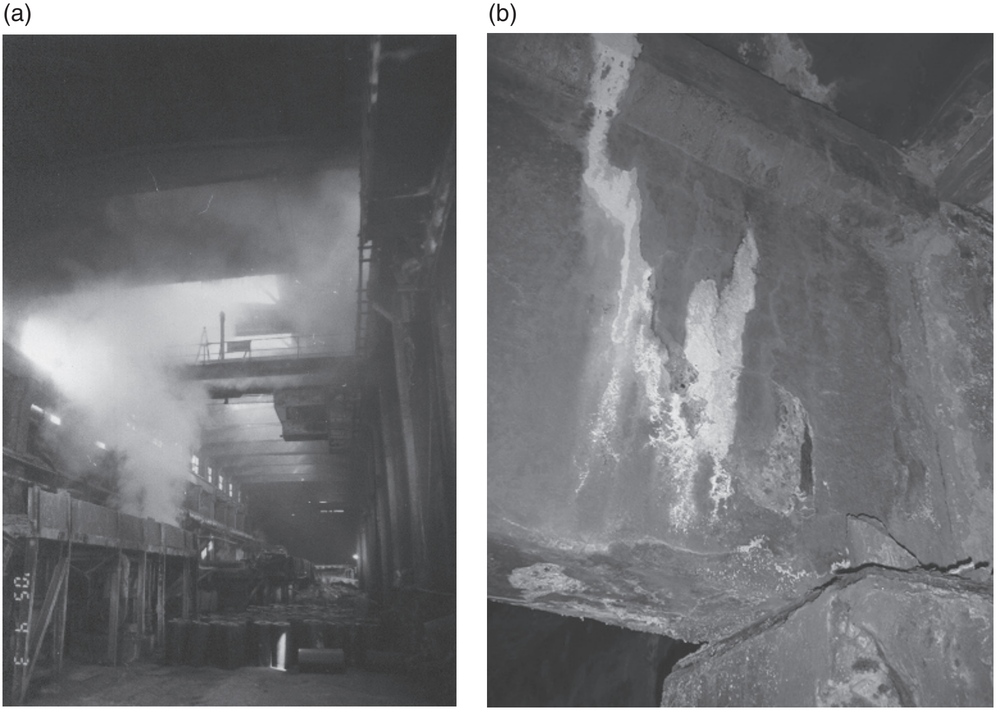

Figure 1.2 Advanced deterioration of concrete elements in a steel process workshop constructed in 1980, aged 24 years at inspection. The RC elements in the steel workshop were exposed to high concentration of corrosive gas rich in chloride and sulfate, high temperature, and humidity (a). The local degradation was manifested through advanced corrosion of steel bars, concrete spalling, and leachates from concrete cracks (b). *Source:* courtesy of Tingyu Hao.

workshops are exposed to high temperature, high humidity and other corrosive gases in addition to CO_2. These corrosive gases can enhance the consumption of CH in pore solution; thus, the deterioration rate of these elements is faster than those exposed to the normal atmosphere. Such an example is presented in Figure 1.2 for a steel process workshop of age 24 years.

Actually, bridge structures on highways, railways, or in urban areas are usually more affected by the deterioration of concrete carbonation due to the total exposure of RC elements to the atmosphere and its thermal and moisture changes. Figure 1.3 illustrates one railway bridge structure of age 26 years seriously affected by the carbonation and the resulted corrosion of the first layer rebars.

Traffic tunnels and underground structures are also affected by concrete carbonation partially due to the fact that CO_2 from traffic exhaust can accumulate to a high level; for example, a value of three times higher than the normal atmospheric CO_2 content (350–380 ppm) has been reported for the Môquet Tunnel in Paris (Ammoura *et al.*, 2014). A full-scale model was built for the subway stations of Shenzhen City, China, in 1999 during the construction phase to demonstrate the long-term performance of different structural concretes of C30 grade. This model was kept in an outdoor environment after the construction and in-situ tests on the drilled cores have been conducted four times since its construction.

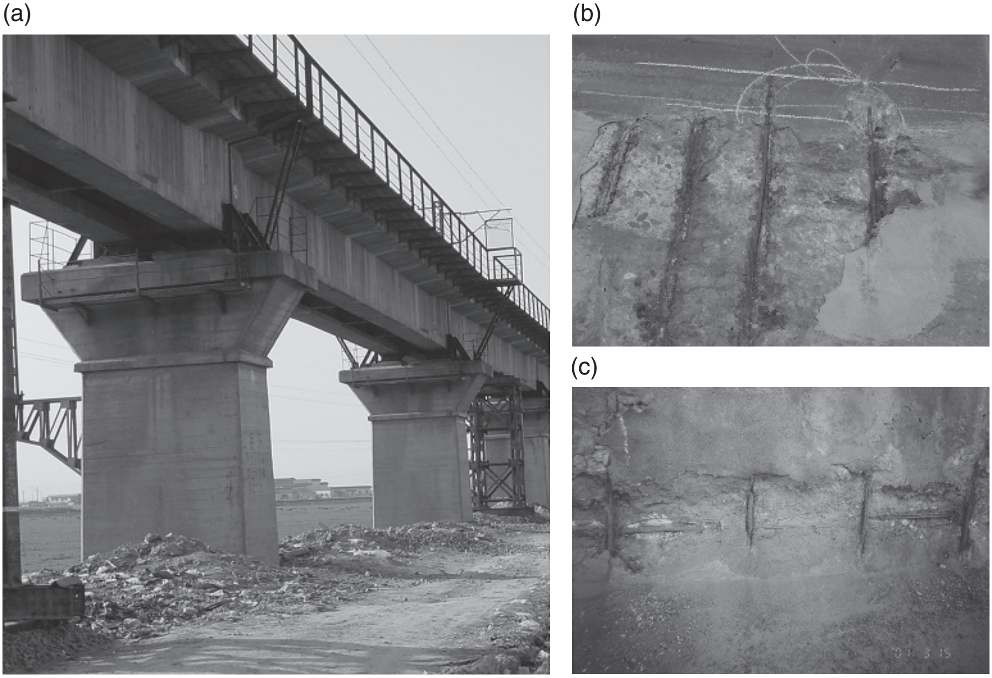

Figure 1.3 Railway bridge after retrofit of the simply supported RC beams (a) and the local corrosion of reinforcement bars by concrete carbonation before the retrofit (b, c). The bridge was constructed in 1976 and the retrofit was finished in 2002. The concrete grade was C50 with OPC as binder, and some local concrete cover was less than 10 mm due to deficient positioning of the reinforcement molds. The bridge is exposed to a typical carbonation environment with an average temperature of 14.6 °C and relative humidity of 56%. *Source:* courtesy of Tingyu Hao.

Figure 1.4 illustrates the inner side of the full-scale model and the carbonation depth measured on the drilled cores from the model walls of age 15 years.

Based on state-of-the-art knowledge of carbonation-induced deterioration and on the experiences of the long-term performance of concrete structures, the favorable conditions for the carbonation deterioration have been well identified: a less-compacted concretes (for carbonation and corrosion), high CO_2 concentrations (for carbonation), and an adequate humidity level (for carbonation and corrosion). It is accepted that the high CH content in concrete is necessary to resist the carbonation of pore solution by infiltrating CO_2, so that a minimum content of 10%, with respect to the binder mass, has been suggested to ensure the carbonation resistance of concrete elements (AFGC, 2007). It is also accepted that the high compactness of concrete helps to limit carbonation by decreasing the CO_2 infiltrating rate and decrease the corrosion risk by increasing the electrical resistivity of concrete. This reasoning favors concretes with both high CH content and high compactness. However, modern concretes increasingly adopt secondary cementitious materials (SCM) in binders, resulting in high compactness of concrete but lower CH content compared with ordinary Portland cement (OPC) binder. For the full-scale model in Figure 1.4, the carbonation depths for OPC concrete ($w/b = 0.56$; binder: OPC 80%, fly ash (FA) 20%) and HPC concrete ($w/b = 0.37$; binder: OPC 36%, FA 36%, granulated blast furnace slag (GGBS) 18%) are respectively 18 mm and 13 mm at an age of 15 years,

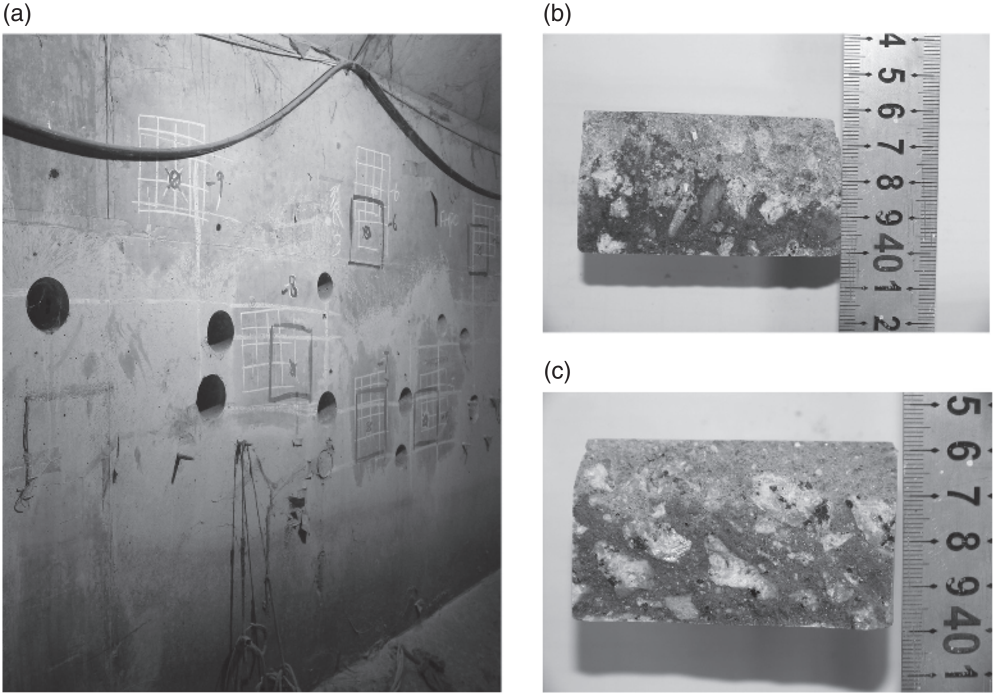

Figure 1.4 Full-scale model for underground station (a) and carbonation depth of wall concrete after 15 years of exposure, 18 mm for OPC concrete (b) and 13 mm for HPC concrete (c). The full-scale model was constructed in 1999 for the long-term observation of different structural concretes used in the subway project of Shenzhen city (average humidity 77%, average temperature 24 °C). *Source:* courtesy of Jianguo Han.

showing that the compactness dominates the CH content with respect to carbonation resistance. Thus, the balance of CH content and the concrete compactness is crucial to making a durable concrete in carbonation environments, particularly for modern concretes incorporating more and more SCM.

1.2 Carbonation of Concrete

1.2.1 Mechanisms

Concrete carbonation includes a series of chemical reactions between the infiltrating CO_2 gas through the material pore space and the liquid interstitial solution in pores. After the hydration of binder materials, the pore solution of hardened concrete contains mainly K^+, Na^+, Ca^{2+} and OH^- ion species and shows high alkalinity, with a pH value around 13.0. Carbonation occurs in the pore solution between the dissolved CO_2 and the aqueous ions species; see Figure 1.5. The preponderant reaction is between CO_2, OH^- and Ca^{2+} as follows:

$$CO_2 + Ca(OH)_2 \rightarrow CaCO_3 \downarrow + H_2O \tag{1.1}$$

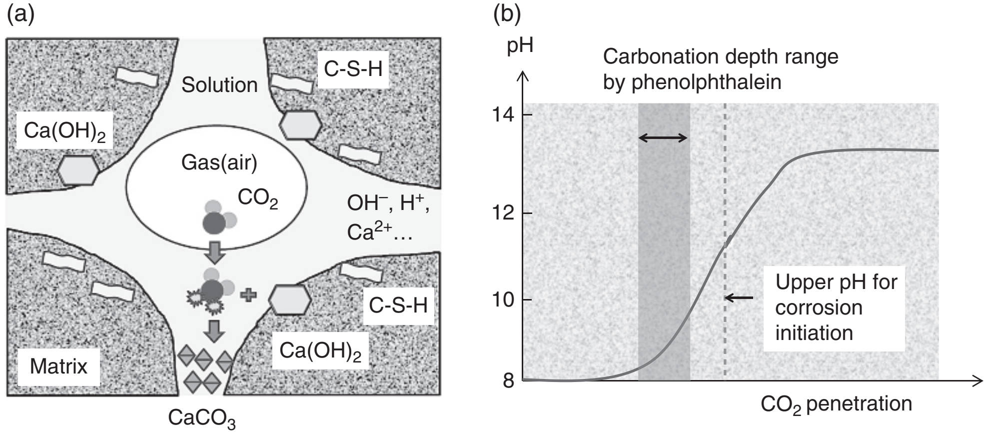

Figure 1.5 Mechanism of carbonation at pore level (a) and pH profile along the CO_2 infiltration direction (b).

Note that this expression masks the dissolution of CO_2 into the pore solution, forming carbonic acid (H_2CO_3) and ionized successively into HCO_3^- and CO_3^{2-}. The results of this reaction are twofold: the consumption of OH^- ions in pore solution and the formation of solid precipitation of calcite ($CaCO_3$) in the pore space. The former decreases the pH value of the pore solution from around 13.0 to below 9.0, while the latter can fill in the original pore space and strengthen the solid matrix of concrete. In the literature, the porosity of carbonated cement pastes with OPC was reported to decrease by 10–15% (Ngala and Page, 1997) and the compressive strength was observed to augment by 30% (Lea, 1970). This knowledge was even used to increase the compactness of hardened concrete by an accelerated carbonation treatment or by introducing CO_2 into the mixing process (Estoup, 1987). However, this compactness effect of CH carbonation is much less in concretes incorporating a large quantity of SCM such as FA or GGBS, and the porosity was even observed to increase. Thus, the beneficial aspect of carbonation on the gain of compactness should be treated with caution.

The CH is not the only phase involved in the reaction with dissolved CO_2 in the pore solution. The C-S-H are the main products from hydration of cement grains and mineral SCM, including actually a group of $(CaO)_x(SiO_2)_y(H_2O)_z$ compounds with Ca/Si ratios varying from 1.2 to 1.7. The solubility of C-S-H is very low in pore solution, and the hydrates can react with the dissolved CO_2, in the form of carbonic acid, forming calcium carbonate and free water (H_2O). According to more detailed research (Dunster, 1989), the carbonation of C-S-H was proposed as follows: the dissolved CO_2 captures calcium ions in C-S-H and leaves anion silicate groups condensed together with lower Ca/Si ratio. In a simplistic way, this reaction was written as (Papadakis *et al.*, 1991b)

$$3CaO \cdot 2SiO_2 \cdot 3H_2O + 3CO_2 \rightarrow 3CaCO_3 \cdot 2SiO_2 \cdot 3H_2O \tag{1.2}$$

Owing to the very low solubility of C-S-H in the pore solution, the influence of C-S-H carbonation on the pH value of the pore solution is regarded as weak. The C-S-H are the main constituents for the solid matrix of cement pastes; thus, the change in C-S-H properties by carbonation can have consequences in concrete materials. Apart from CH and C-S-H, other minerals in hardened cement paste can also react with dissolved CO_2 in the pore solution, including the unhydrated minerals of tricalcium silicates (C_3S) and dicalcium silicates (C_2S) and aluminates hydrates. And the carbonation of aluminate hydrates is thought to be rapid (Thiery, 2005).

As CO_2 migrates into the pores, the above reactions occur simultaneously with the dissolution of CO_2 from the gas phase into the aqueous phase; see Figure 1.5. In engineering practice, the carbonation depth is usually measured by phenolphthalein ($C_{20}H_{14}O_4$) solution, in 1% mass concentration. The phenolphthalein solution remains colorless for low pH value and turns to a pink–red color for high pH value, and the color change point of pH value is around 9.0. The solution is spayed on the exposed surface, fractured or drilled, and the pink–red zone is assumed to mark the boundary between the carbonated and intact zones. Nowadays, this carbonation depth is widely adopted as the indicator of carbonation extent of concrete. However, the approximate nature of this characterization should be borne in mind: the phenolphthalein solution changes its color over a pH range – that is, between 8.4 and 9.8 (McPolin *et al.*, 2009) – and the pH value of the pore solution along the CO_2 infiltration direction follows a gradual change rather than a steep front; see Figure 1.5. Nevertheless, the concept of carbonation front is still used in the modeling in this chapter owing to its simplicity.

1.2.2 Influential Factors

Concrete carbonation is fundamentally affected by two aspects: the material intrinsic properties involved in the carbonation reactions and the external environmental factors. The material properties include, on the chemical side, the content of reactive hydrates (CH, C-S-H, C_3S, C_2S and aluminates hydrates) in the solid phase, and the resistance of the pore structure to CO_2 infiltration on the physical side. The external factors refer to the atmospheric CO_2 concentration, the temperature and the environmental humidity.

CH Content and CO_2 Diffusivity

The CH content of hardened cement-based materials is the result of the hydration reaction between the binder materials and mixing water, related closely to the chemical composition and hydration extent of the binder materials. Figure 1.6 shows the CH content of cement pastes using OPC as the only binder material for different *w/c* ratios. The CO_2 infiltration is resisted by the tortuous pore structure of concrete and the pore solution as well since CO_2 can only transport in the gas-occupied space. Taking the diffusivity of CO_2 in concrete to characterize the infiltration rate, several analytical expressions were proposed for the diffusivity in terms of the porosity and environmental humidity. Papadakis *et al.* (1991a) proposed the expression

$$D_{CO_2} = 1.64 \times 10^{-6} \phi_p^{1.8} (1-h)^{2.2} \tag{1.3}$$

where D_{CO_2} (m^2/s) is CO_2 diffusivity, ϕ_p is the porosity of cement-based materials, and h is the relative humidity in the environment. Using the same data sets, the above relation was

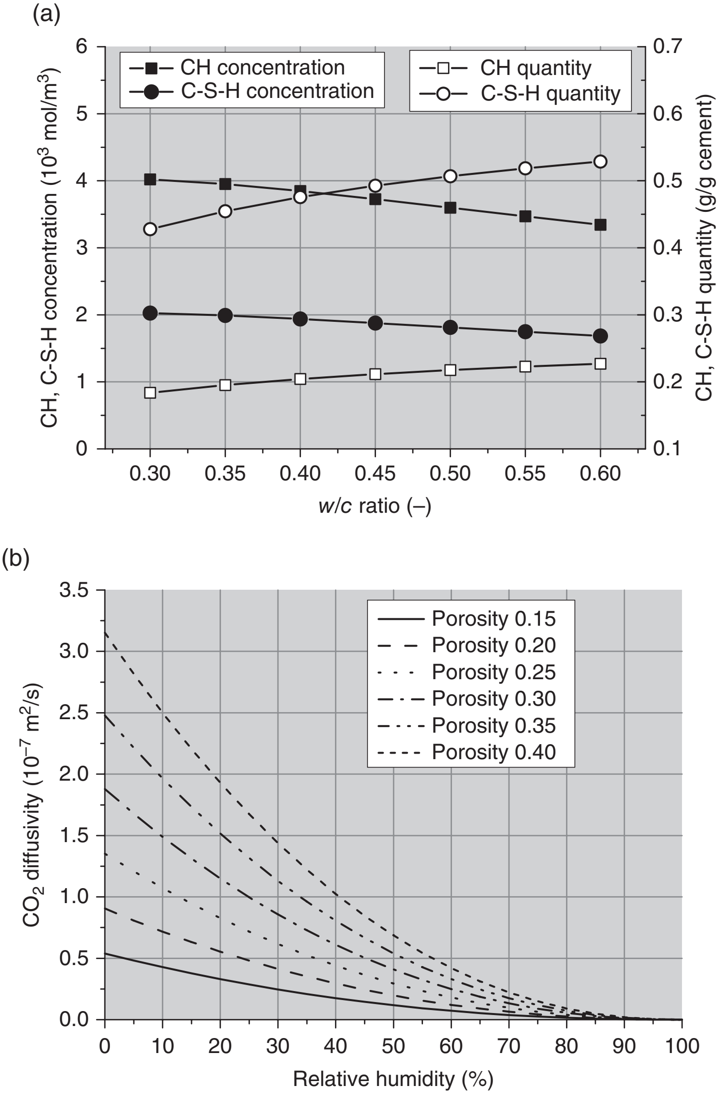

Figure 1.6 CH content for OPC pastes with different *w*/*c* ratios (a) and CO_2 diffusivity in terms of porosity and environmental humidity using Equation 1.3 (b). The simplified hydration model from Papadakis *et al*. (1991a) is retained and the CH/C-S-H contents are first evaluated for a totally hydrated state. Then, the hydration extent is estimated for different *w*/*c* ratios using the model from Lam *et al*. (2000), and the stable CH/C-S-H contents are estimated from the total contents and the hydration extents.

calibrated in terms of the CO_2 diffusivity in air $D^0_{CO_2}$, total porosity of concrete ϕ, and the pore saturation s_1 as (Thiery, 2005)

$$D_{CO_2} = D^0_{CO_2}\phi^{2.74}\left(1-s_1\right)^{4.20} \tag{1.4}$$

with $D^0_{CO_2}$ equal to 1.6 × 10^{-5} m^2/s at 25 °C. The CEB-FIP model code (CEB, 1990) proposed a value range (0.5–6) × 10^{-8} m^2/s for hardened concretes and related the diffusivity to the characteristic value of compressive strength f_{ck} (MPa) through

$$-\log D_{CO_2} = 7.0 + 0.025 f_{ck} \tag{1.5}$$

This expression was prescribed for concrete elements sheltered from rain, corresponding roughly to a relative humidity $h = 60\%$.

CO_2 Concentration, Temperature and Humidity

The CO_2 concentration in the surrounding environment of concrete structures plays an important role in the carbonation process. If the kinetics of carbonation are assumed to be controlled by the CO_2 diffusion, then the carbonation depth will be proportional to the square root of the CO_2 concentration in the environment (DuraCrete, 2000). In other words, augmenting CO_2 concentration by 25% leads to an increase of carbonation depth by 12% for concrete. The concentration in the atmosphere is normally in the range 350–380 ppm, corresponding to 0.57–0.62 g/m^3. Owing to greenhouse gas emissions in recent decades, the CO_2 concentration in the atmosphere has augmented from 280 ppm in 1750 to 380 ppm in 2005 (IPCC, 2007). Compared with the average atmospheric value, the local CO_2 concentration surrounding a particular structural element can be much higher: it can readily double the average value in less-ventilated conditions and adopt even higher values in polluted urban areas.

The temperature is another basic factor for concrete carbonation in the natural environment. Coupled with the greenhouse emission process, the atmospheric temperature is found to have increased from 0.074 °C per decade in the past 100 years to 0.177 °C per decade in the past 25 years (IPCC, 2007). For service lives of 50–100 years, this global warming gives a rather moderate augmentation. Again, the local climate has much more influence on the temperature for concrete structures. A higher temperature is expected to accelerate the carbonation since all the reactions involved are by nature electrolytic and thermally activated. But note that the solubility of CO_2 in the pore solution is also reduced at a higher temperature. Owing to these two opposite effects, the influence of temperature on carbonation rate is considered not important (Chaussadent, 1999). Contrary to the temperature, the environmental humidity has a very distinct impact on the carbonation process: low humidity leaves more pore space for CO_2 infiltration, but the dissolved CH quantity in the pore solution is limited by the low pore saturation; the high humidity increases the pore saturation and thus hinders directly the CO_2 transport; the optimum humidity range was found to be between 50 and 70%. A nominal value of $h_{opt} = 65\%$ was adopted and a factor k_e was proposed for the influence of humidity on the carbonation process (*fib*, 2006):

$$k_e = \left(\frac{1 - h^f}{1 - h^f_{opt}} \right)^g \tag{1.6}$$

with f and g as model parameters, adopting $f = 5.0$ and $g = 2.5$. Note that this expression gives a conservative prediction for $h < h_{opt}$.

Accelerated Carbonation

Setting the CO_2 concentration and relative humidity level, the carbonation can be accelerated substantially in the laboratory. Actually, accelerated tests have been established to characterize the carbonation resistance of concrete in the laboratory. The principle of these tests is to put concrete specimens under high CO_2 concentration of 2–50% and humidity $h = 60 - 70\%$ and measure the carbonation depth by phenolphthalein solution for a given duration. The measured carbonation depth, or the carbonation resistance deduced from the carbonation depth, is regarded as a useful durability indicator for concrete exposed to a carbonation environment. Theoretically, the difference between the accelerated carbonation (ACC) and natural carbonation (NAC) is due to the environmental conditions; that is, CO_2 concentration and humidity level. However, since the NAC occurs during a time span much longer than the ACC, the intervention of other processes, such as natural drying and the long-term microstructure evolution of concrete, is inevitable and difficult to quantify. Figure 1.7 illustrates the correlation between ACC and NAC at the exposure site in Maurienne, France (Baroghel-Bouny *et al.* 2004). The correlation seems stronger for concrete with strength higher than 25 MPa and weaker for lower strength concretes.

1.2.3 Models

On the basis of theoretical and experimental investigations of concrete carbonation, various models have been proposed in the literature, and the reference (DuraCrete, 1998) provides a comprehensive description for the available models on carbonation depth in its Appendix A.

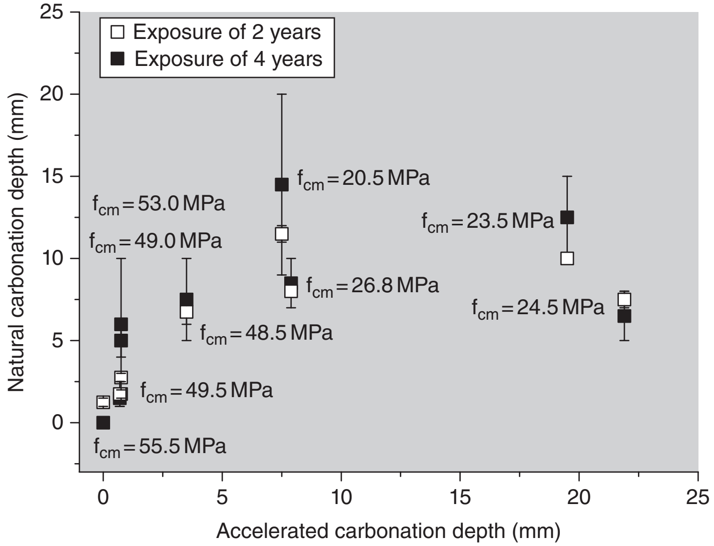

Figure 1.7 Correlation between ACC and NAC of structural concretes. Data were taken from Baroghel-Bouny *et al.* (2004: tables VIII and X). The ACC tests were performed under a CO_2 concentration of 50% for 14 days' duration. The annual average temperature was recorded as between 7.5 and 11.1 °C. f_{cm}: compressive strength.

Here, only two models are introduced: the mechanism-based model (C-1) from Papadakis *et al.* (1991b) and the empirical model (C-2) from *fib* (2006) model code. Both models use the concept of carbonation front and take into account the main influential factors described in Section 1.2.2.

Model C-1

Papadakis *et al.* (1991b) provided the mathematical model for the carbonation depth on the basis of simplified carbonation mechanisms: the cement hydrates that participate in the carbonation reaction include CH, C-S-H and C_3S, C_2S in the unhydrated cement grains. The mass conservation of CO_2 gas considering these carbonation reactions is

$$\frac{\partial}{\partial t}\left(\phi\left(1-s_1\right)\left[\mathrm{CO_2}\right]\right)=\frac{\partial}{\partial x}\left(D_{\mathrm{CO_2}}\frac{\partial\left[\mathrm{CO_2}\right]}{\partial x}\right)-\phi_0 s_{\mathrm{w}} r_{\mathrm{CH}}-3r_{\mathrm{CSH}}-3r_{\mathrm{C_3S}}-2r_{\mathrm{C_2S}} \tag{1.7}$$

where ϕ and ϕ_0 are the porosities of concrete after and before the carbonation, $[CO_2]$ (mol/m^3) is the CO_2 concentration, s_1 and s_w are respectively the porosity occupied by the liquid phase and the porosity filled with water,[1] r_x (mol/s) (x = CH, CSH, C_3S, C_2S) are the reaction rates of these reactants with CO_2, and the coefficients before these reaction rates are the corresponding stoichiometric constants in the respective carbonation reactions. If the hydrates are stable and no more hydration reactions consume or produce these reactants, these reactions rates are equal to the mass change rate of these compounds:

$$\frac{\partial}{\partial t}[\mathrm{CH}]=-\phi_0 s_{\mathrm{w}} r_{\mathrm{CH}},\qquad \frac{\partial}{\partial t}[\mathrm{CSH}]=-r_{\mathrm{CSH}},\qquad \frac{\partial}{\partial t}[\mathrm{C_3S}]=-r_{\mathrm{C_3S}},\qquad \frac{\partial}{\partial t}[\mathrm{C_2S}]=-r_{\mathrm{C_2S}} \tag{1.8}$$

where [CH], [CSH], $[C_3S]$, and $[C_2S]$ (mol/m^3) are the reactant contents in concrete. Now suppose the carbonation advances into concrete through a carbonation "front"; see Figure 1.8. The position of this front is denoted by x_c. At the right side of the carbonation front, $x > x_c$, all the reactants (CH, C-S-H, C_3S, and C_2S) are assumed to be intact, taking their initial contents $[CH, CSH, C_3S, C_2S]^0$; but all these reactants are totally consumed by the carbonation reactions; that is, $[CH, CSH, C_3S, C_2S] = 0$ as $x < x_c$. In the carbonation range the CO_2 is assumed to be in steady state; that is:

$$\frac{\partial}{\partial t}\left(\phi\left(1-s_1\right)\left[\mathrm{CO_2}\right]\right)=0 \quad \text{for} \quad 0<x<x_{\mathrm{c}} \tag{1.9}$$

Under a constant CO_2 concentration imposed on the concrete surface, $x = 0$, this assumption leads to a linear distribution of CO_2 in the carbonation range; that is, $[CO_2] = [CO_2]^0(1 - x/x_c)$.

---

[1] The difference lies in the assumption that, under a certain environmental humidity, the pores with size smaller than the size at equilibrium with a humidity through the Kelvin equation are filled by liquid water, denoted by s_w, and the pores above this size contain a water film on the pore wall. The total liquid saturation s_1 is the sum of the water-filled porosity and the volume of water films.

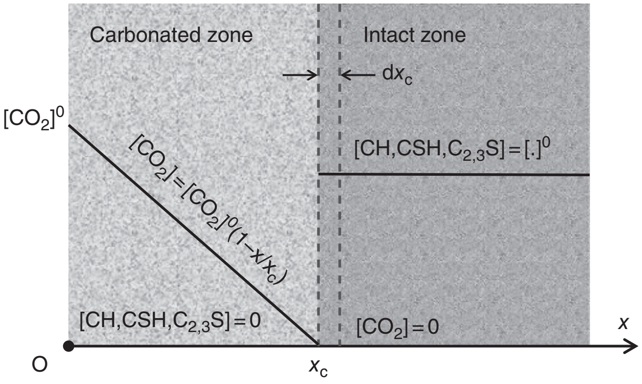

Figure 1.8 Schematic illustration of the C-1 model for carbonation depth.

Now focus on the CO_2 mass conservation as the carbonation front moves from x_c to $x_c + dx_c$. The conservation in Equation 1.7, considering Equations 1.8 and 1.9, becomes

$$-\left(D_{CO_2}\frac{\partial[CO_2]}{\partial x}\right)_{x_c}^{x_c+dx_c} = \frac{dx_c}{dt}\left([CH]+3[CSH]+3[C_3S]+2[C_2S]\right)_{x_c}^{x_c+dx_c} \tag{1.10}$$

Using the linear distribution of CO_2 concentration, this relation turns to

$$x_c\frac{dx_c}{dt} = \frac{D_{CO_2}[CO_2]^0}{[CH]^0+3[CSH]^0+3[C_3S]^0+2[C_2S]^0} \tag{1.11}$$

After integration, the carbonation depth is written as

$$\begin{aligned} x_c &= x_c^0 + \sqrt{\frac{2D_{CO_2}[CO_2]^0}{[CH]^0+3[CSH]^0+3[C_3S]^0+2[C_2S]^0}t} \\ &= x_c^0 + k_{carb}\sqrt{t} \end{aligned} \tag{1.12}$$

where x_c^0 (m) is the initial carbonation depth corresponding to $t = 0$, D_{CO_2} (m^2/s) is the CO_2 diffusivity in concrete expressed in terms of the porosity and the pore saturation or relative humidity (see Equation 1.3 or 1.4), and $[CO_2]^0$ (mol/m^3) is the atmospheric CO_2 concentration to which the concrete is exposed. This model gives a carbonation depth proportional to the square root of exposure time t. This proportionality has been confirmed by experiments as well as in-field investigations. This model has clear carbonation mechanisms behind it and has been used extensively in research and applications.

However, several aspects are to be considered in applying this model to structural concrete carbonation. First, this model should be applied to concrete in its totally hardened state so that Equation 1.8 can be observed. Second, the concentration of reactants near the carbonation front in Equation 1.10 is greatly simplified, and this simplification, in addition to the carbonation front concept, gives an approximate nature for the carbonation depth predicted by Equation 1.12. Third, the concentrations of CH, C-S-H, C_3S, and C_2S depend much on the cement composition and the hydration extent in concrete; unless accurately quantified, the estimation of these concentrations always introduces errors into the prediction results. Further, the carbonation reaction is also simplified with respect to C-S-H using a constant Ca/Si ratio in Equation 1.2; this assumption can be acceptable for concretes using OPC but is less valid for concretes incorporating SCMs. Finally, the carbonation depth in this model corresponds to the position where all reactant are consumed; thus, the local pH value at the carbonation front will be lower than the color change point of the phenolphthalein solution (i.e., pH 8.4).

The model parameters are summarized in Table 1.1, and some usual values are provided for the initial mineral contents in cement hydrates using the results in Figure 1.6 and assuming a volumetric volume ratio of 0.35 for cement paste in concrete. On the basis of these parameters and relations, simulation results are given in Figure 1.9 for carbonation depths in terms of the concrete porosity and environmental humidity. For comparison, two cases are presented: carbonation with CH and C-S-H, and carbonation with only CH. The results show the dominating impact of humidity on the carbonation depth and the contribution of C-S-H to the carbonation resistance; that is, the carbonation depth for the CH + C-S-H case is 30–50% smaller than for the CH case. With the simplification in Equation 1.2 for C-S-H carbonation, the predictions from these two cases can actually be used as boundary values for engineering applications.

Note that the above results are computed for concretes using 100% OPC as binder materials. Incorporating mineral admixtures, such as pozzolanic materials, can decrease substantially the CH content in hardened concrete. In that case, the CH and C-S-H cannot be taken directly from Table 1.1 or Figure 1.6, but from more specified hydration models or direct experimental characterizations.

Model C-2

Following a very engineering approach, the *fib* (2006) model code proposed an empirical model for carbonation depth on the basis of the ACC results, taking into account the environmental and the curing conditions of concrete. The carbonation depth is expressed through

$$x_c(t) = \sqrt{2k_e k_c R_{\mathrm{NAC}}^{-1} C_{\mathrm{CO_2}}}\sqrt{t}W_t \tag{1.13}$$

Table 1.1 Model parameters for the C-1 model and their usual value ranges

Parameter (unit)	Value/relation
CH content in concrete $[\mathrm{CH}]^0$ (10^3 mol/m^3)	1.17–1.41 from Figure 1.6
C-S-H content in concrete $[\mathrm{CSH}]^0$ (10^3 mol/m^3)	0.590–0.709 from Figure 1.6
C_3S content in concrete $[C_3S]^0$ (mol/m^3)	0 for total hydration state
C_2S content in concrete $[C_2S]^0$ (mol/m^3)	0 for total hydration state
CO_2 concentration in atmosphere $[CO_2]^0$ (mol/m^3)	0.0147–0.0295 (400–800 ppm)
CO_2 diffusion coefficient in concrete $D_{\mathrm{CO_2}}$ (m^2/s)	Equation 1.3 or 1.4
Porosity of concrete ϕ	0.09–0.18 ($w/c = 0.30 - 0.60$)
Relative humidity (%)	0–100
Initial carbonation depth x_c^0 (m)	0–0.01

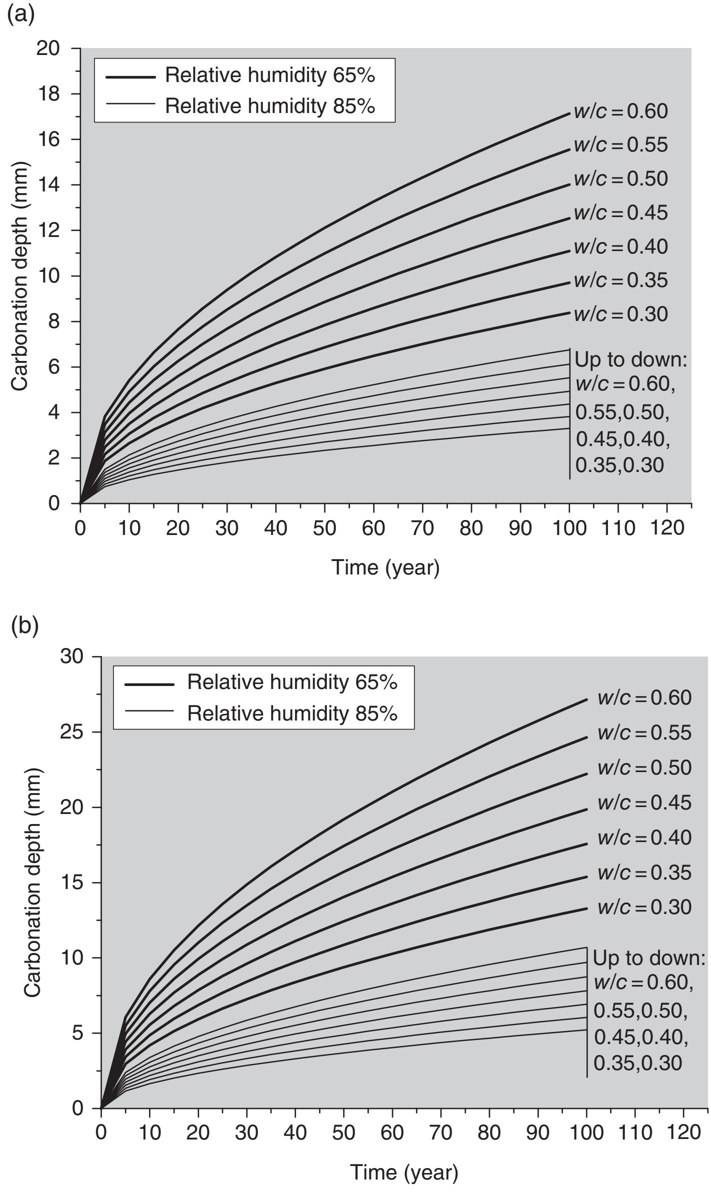

Figure 1.9 Carbonation depth from the C-1 model for concretes under different relative humidity: model results considering CH and C-S-H carbonation (a) and model results considering only CH carbonation (b). The CO_2 concentration is 0.0184 mol/m^3, corresponding to 500 ppm.

where k_e is the environmental factor considering the relative humidity and further the pore saturation of concrete (and its value can be evaluated from Equation 1.6); k_c is the curing factor reflecting the hardening extent of concrete as exposed to the atmosphere, taking the form

$$k_c = \left(\frac{t_c}{7}\right)^{b_c} \tag{1.14}$$

with t_c (days) as the curing duration of concrete and b_c the regression exponent. R_{NAC}^{-1} (m^2/s per kg CO$_2$/m^3, or mm^2/a per kg CO$_2$/m^3) is the resistance of concrete to carbonation in natural exposure under a reference relative humidity of 65%, and can be related to the ratio between the binding capacity of CO_2 in concrete (kg CO$_2$/m^3) and the effective diffusion coefficient of CO_2 in concrete (m^2/s or mm^2/a) (*fib*, 2006). This quantity is related to the ACC test[2] through the relation

$$R_{NAC}^{-1} = k_t R_{ACC}^{-1} + \varepsilon_t \tag{1.15}$$

where k_t and ε_t (m^2/s per kg CO$_2$/m^3, mm^2/a per kg CO$_2$/m^3) are regressed parameters. This relation issues from the correlation analysis between the NAC resistance of concrete and the resistance under the ACC test. The resistance R_{ACC}^{-1} was tested for various binders (composition and *w*/*b* ratio) and the recommended values are given in Table 1.2. C_{CO_2} is the CO_2

Table 1.2 Model parameters for the C-2 model and their usual value ranges

Parameter (unit)	Value/relation	Uncertainty range (%)
Environmental factor f_e	1.0 (65%), 0.31 (85%)	n.d.
Curing condition factor f_c	3.0 (1 day), 1.61 (3 days), 1.0 (7 days), 0.77 (11 days), 0.67 (14 days)	n.d.
Regression parameter k_t	1.25	28
Regression parameter ε_t (mm^2/a per kg CO$_2$/m^3)	315.5	15
$R_{ACC}^{-1}(w/b)$ (10^3 mm^2/a per kg CO$_2$/m^3) Binder: CEM I R42.5	0.98 (0.40), 1.64 (0.45), 2.14 (0.50), 3.09 (0.55), 4.22 (0.60)	4
$R_{ACC}^{-1}(w/b)$ (10^3 mm^2/a per kg CO$_2$/m^3) Binder: CEM I + FA (20%)	0.95 (0.40), 0.60 (0.45), 0.76 (0.50), 2.05 (0.55), 2.62 (0.60)	40
$R_{ACC}^{-1}(w/b)$ (mm^2/a per kg CO$_2$/m^3) Binder: CEM III/B	2.61(0.40), 5.32(0.45), 8.38(0.50), 13.95(0.55), 25.20(0.60)	25
C_{CO_2} (10^{-3} kg/m^3)	0.82 (500 ppm)	12
Weather exponent w	0.0 (indoors), 0.13, 0.21 (outdoors)	n.d.
Weather factor W_t	1.0 (indoors), 1.16 (outdoors)	n.d.

---

[2] This ACC test is after the experimental procedure from the DARTS project (DARTS, 2004). The concrete specimens undergo 6 days' curing in water and 21 days' curing under 20 °C and 65% humidity. Then the specimens are subject to a carbonation test with 2% CO_2 concentration for 28 days, and the carbonation chamber is controlled to 20 °C and 65% humidity.

concentration in the atmosphere (kg CO_2/m^3). The conventional value can be adopted as 0.82×10^{-3} kg/m^3, corresponding to a concentration of 500 ppm in air. Note that the average CO_2 concentration in the atmosphere is between 350 and 380 ppm. W_t is the weather coefficient considering the influence of the wetting by precipitation on the concrete carbonation, expressed as

$$W_t = \left(\frac{t_0}{t}\right)^w \tag{1.16}$$

The reference time t_0 refers to the standard age for concrete under the ACC test (28 days), and the exponent w is determined by the time of wetness and the probability of driving rain (*fib*, 2006). This factor makes the difference between the indoor and outdoor exposure conditions, and some typical values are calculated and presented in Table 1.2.

This model is more adapted to engineering use since no chemical parameters are involved. The compactness of concrete is considered through the inverse carbonation resistance R_{NAC}^{-1} and related to the laboratory ACC test. The influence of humidity on carbonation is addressed through the environmental factor k_{e} and the weather factor W_t. Moreover, the crucial influence of curing age on concrete carbonation is included through the factor f_{c}. Some further studies linked the NAC resistance R_{NAC}^{-1} with the concrete compressive strength (Guiglia and Taliano, 2013). Moreover, the uncertainty associated with the parameters in this model was also quantified, which is important in evaluating the reliability of model prediction.

The drawback of this model comes from the relationship in Equation 1.15. Actually the credibility of the model hinges on this equation, which links the NAC resistance with ACC resistance. The ACC test follows a particular procedure, including curing and drying on concrete specimens and the CO_2 concentration/relative humidity level in the carbonation chamber. This particularity limits the possibility of more extensive model calibration for concretes with different binder materials, though a relatively complete study was done on different binders.

The main parameters in the model are summarized in Table 1.2. On the basis of these values, simulations are performed for the carbonation depth for the usual ranges of concrete carbonation resistance and weather conditions in Figure 1.10.

1.3 Steel Corrosion by Carbonation

1.3.1 Mechanism

Carbonation consumes OH^- ions in the pore solution, and the electrochemical stability of embedded steel bars is affected. The electrochemical stability of the reinforcement steel can be described by the Pourbaix diagram of iron in water, which illustrates the thermodynamic equilibrium between the iron and its ion and oxide species; see Figure 1.11. On the figure, several zones are identified for iron in the Fe–H_2O system: immune zone, passivation zone, and corrosion zone. The pore solution of concrete without carbonation usually has a pH value in the range 12.4–13.2, situating the iron in the immune–passivation zones. In other words, a passivation film is formed on the steel surface.

As the pH value of the pore solution is decreased by carbonation, this passivation film is destroyed and the anode reaction of corrosion can occur, turning Fe to Fe^{2+}. This phase is

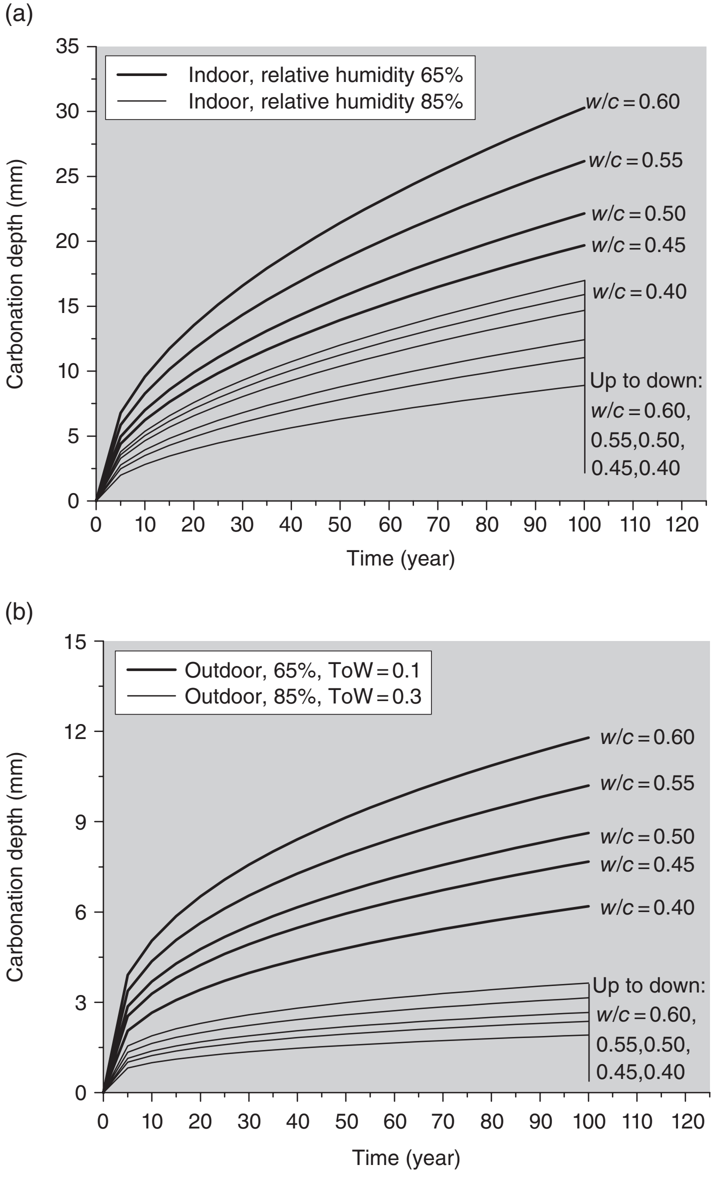

Figure 1.10 Carbonation depth from the C-2 model for OPC concrete with different *w*/*b* ratios for indoor exposure (a) and outdoor exposure (b). For the outdoor exposure, two cases are studied: one for the time of wetness ToW = 0.1 and driving rain probability p_{SR} = 0.5, and the other case for ToW = 0.3 and p_{SR} = 0.5. The former is representative of a dry climate and the latter of a wet climate.

termed the "corrosion initiation" for carbonation-induced corrosion. As mentioned before, the concept of carbonation depth is used to simplify the engineering judgement of carbonation extent, and the profile of pH value actually follows a gradual change along the carbonation depth; see Figure 1.5. Thus, the position of carbonation depth, determined by phenolphthalein

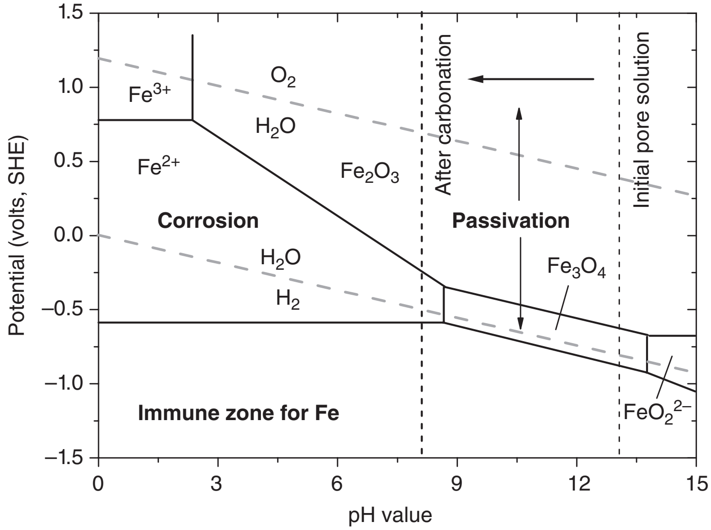

Figure 1.11 Pourbaix diagram for Fe–H_2O system at 25 °C (note that the accurate position of the lines drawn depends on the concentration of the ions, and the ion concentration is taken as 10^{-6} M). *Source:* adapted from Kośmider 2011, Wikimedia Commons, Public domain.

solution, cannot accurately capture the pH value condition for corrosion initiation. Actually, both laboratory research and in-field investigations revealed that the steel corrosion can be initiated before the carbonation depth (quantified by the phenolphthalein solution) reaches the steel surface. This distance was termed “residual depth of carbonation” or “carbonation remains,” and this value was observed as 5.8–27 mm for a cover thickness of 16.9–50 mm for outdoor concrete elements (Dong *et al.*, 2006). But note that this residual depth adopted negative values for indoor exposure from the same data set; that is, −16 to +5.3 mm for concrete cover of 20–40 mm.

Once initiated, the electrochemical process of corrosion consists of anode and cathode reactions: the Fe atoms lose electrons at the anode and turn into Fe^{2+} ions; the electrons, oxygen and water form OH^- ions at cathode; and the OH^- ions formed flow back to the anode to produce $Fe(OH)_2$ or $Fe(OH)_3$ compounds and deposit as solid phases (rust). The intensity of the electrochemical process can be quantified by the electrical current density, or corrosion rate I_{corr}, between the anode and cathode. The corrosion rate is controlled by both the electrical resistance of the concrete and the cathode reaction: when the pore saturation is low (e.g. the corresponding relative humidity lower than 90%), the corrosion rate is controlled by the concrete resistivity since the OH^- ions must flow back to the anode to close the electrical circuit through the concrete around the steel; when the pore saturation is high (e.g. the relative humidity higher than 95%), the diffusion of oxygen to the cathode controls the whole process; for a pore saturation in between there exists a transition from resistance-controlled mechanism to a cathode-reaction-controlled one (Raupach, 2006). Under carbonation, the corrosion is a general corrosion type; that is, the anodes and cathodes are evenly distributed on the steel surface and the anode and cathode are regarded as having comparable sizes.

The corresponding anode/cathode ratio is usually considered as 1.0 in models for corrosion current evaluation (Yu *et al.*, 2014).

1.3.2 Influential Factors

The target parameter for the steel corrosion is the corrosion current density I_{corr} hereafter. Admittedly, the first influential factor for the steel corrosion is the electrochemical property of steel itself. Incorporating some metal elements like chromium (Cr) and nickel (Ni) will greatly increase the corrosion resistance of steel, but this section treats only reinforcement steel bars made from conventional carbon steel (black carbon steel). Thus, the electrochemical properties of steel are not included as influential factors.

Temperature and Humidity

The influential factors of environmental conditions refer to the relative humidity and the ambient temperature. The relative humidity determines the pore saturation of concrete, and thus the corrosion mode. This influence is determinant for corrosion current: as the pore saturation increases with the relative humidity, the corrosion mode changes from a resistance-controlled one to a cathode-reaction-controlled one. The range of corrosion mode change is estimated as 90–95% in terms of environmental relative humidity (Yu *et al.*, 2014). Accordingly, given the concrete quality and cover thickness, the corrosion current is to increase firstly with the pore saturation due to the reduced electrical resistance, reaching a maximum around $h = 90\%$, and then to decrease with the pore saturation due to the slower oxygen diffusion to the cathode. The ambient temperature is believed to play a role in the corrosion rate of reinforced steel, since both the electrochemical reactions and the oxygen diffusion are influenced by ambient temperature. Tuutti (1982) reported a logarithmic rise of corrosion rate for carbonated concrete specimens for the temperature range −20 to +30 °C. Thus, the ambient temperature should be taken into account for engineering application.

Concrete Cover

The concrete cover has a determinant impact on the corrosion current through its thickness, compactness, and pore saturation. The influence of pore saturation has been considered through the environmental relative humidity. The thickness of concrete cover has a different impact on the two corrosion modes: for the resistance-controlled mode the thickness can contribute to the electrical current path and thus the current increases with concrete cover, but this increase is estimated to be rather moderate; for the cathode-reaction-controlled mode the thickness delays the oxygen diffusion and thus reduces the corrosion current. The compactness of concrete influences the corrosion rate in the resistance-controlled mode through the concrete resistivity, and the corrosion rate in the cathode-reaction-controlled mode through the diffusivity for oxygen. For both modes, high compactness of concrete helps to reduce the corrosion current. In some studies the compactness of concrete was denoted by the *w*/*c* (*w*/*b*) ratio of the concrete mixture. Note that the compactness of structural concrete can also evolve due to the further hydration of cementitious materials, particularly for those concretes incorporating a large quantity of SCM.

Concrete–Steel Interface

Another factor involved in the corrosion current is the quality of the concrete–steel interface and its impact on the corrosion process. So far, the steel corrosion induced by the carbonation of concrete cover assumes a perfect adhesion between the concrete and steel. Actually, the interface can contain heterogeneous defects, and these defects can change the corrosion initiation time and corrosion rates (Nasser *et al.*, 2010). The impact of concrete–steel interface quality on the corrosion process is still to be quantified.

1.3.3 Models

The aforementioned knowledge on the initiation of steel corrosion by carbonation and the corrosion current allows the establishing of practical models on corrosion initiation and electrical current for engineering use. Two models are presented for corrosion initiation and corrosion current in the following.

Model C-3: Corrosion Initiation by Carbonation

Corrosion initiation has been conventionally taken as the carbonation depth reaching the surface of reinforcement bars. However, owing to the simplistic nature of the carbonation front concept and the approximate nature of carbonation depth measured by phenolphthalein solution, the initiation condition can be more appropriately expressed as

$$x_{\mathrm{c}} - \Delta x_{\mathrm{c}} \geq x_{\mathrm{d}} \tag{1.17}$$

with Δx_{c} (m) the residual carbonation depth and x_{d} (m) the concrete cover thickness to the reinforcement bars. This residual depth accounts for the fact that the corrosion can be already initiated before the carbonation depth (detected by phenolphthalein solution) reaches the steel surface. The residual carbonation depth can take the following expression, adapted from the CECS technical standard (CECS 2007),

$$\Delta x_{\mathrm{c}} = \left(1.2 - 0.35\sqrt{k_{\mathrm{carb}}}\right) x_{\mathrm{d}} - 1.94 k_{\mathrm{carb}} - 3.46 \quad \text{with} \quad k_{\mathrm{carb}} = \frac{x_{\mathrm{c}}}{\sqrt{t}} \tag{1.18}$$

with x_{c}, Δx_{c}, and x_{d} in millimeters and t in years. The carbonation rate coefficient k_{carb} (mm/a$^{0.5}$) in this expression is defined as the ratio between the carbonation depth x_{c} and the square root of exposure age at measurement. Note that this model was regressed from 120 RC elements from 18 cities in China with the concrete cover thickness ranging from 20 to 50 mm. No dispersion analysis is available for this model. Taking the measured value range for k_{carb}, the carbonation residual depth is illustrated in Figure 1.12 for different values of cover thickness.

Model C-4: Corrosion Current

Once initiated, the corrosion develops with a certain density of corrosion current. From the mechanisms for steel corrosion, the model should include the resistance-controlled mode and cathode-reaction-controlled mode of steel corrosion in concrete. However, few models in the

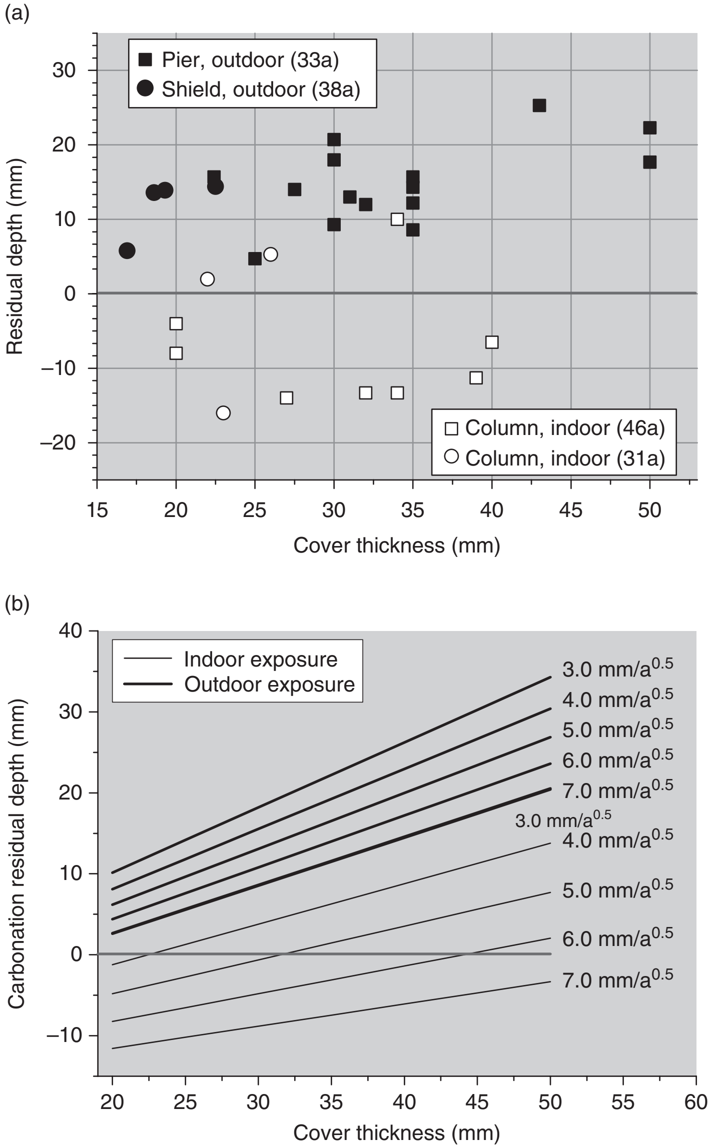

Figure 1.12 Residual carbonation depth measured from in-situ RC elements (a) and predicted from model C-3 in terms of the ratio k_{carb} (3.0–7.0 mm/a$^{0.5}$) and cover thickness (b). Image (a) is generated from data taken from Dong *et al*. (2006: table 2). The residual depth on the figure is for $W_t = 1.0$ and 0.426 for indoor and outdoor conditions, and the outdoor value corresponds to ToW = 0.1 and $p_{\text{SR}} = 0.5$ in Figure 1.10.

literature can account for both mechanisms and properly describe the influence of both environmental factors and concrete properties. Accordingly, a simplified model is retained here considering mainly the resistance-controlled corrosion. The electrical current density of corrosion I_{corr} (A/m^2) is expressed through

$$I_{\text{corr}} = \frac{V_0}{\rho} \tag{1.19}$$

where V_0 (V/m) is a reference potential gradient and ρ (Ω m) is the electrical resistivity of the concrete cover. Following the DuraCrete model (DuraCrete, 2000), the reference potential gradient is taken as 0.76 V/m. The concrete resistivity ρ depends on the pore saturation (environmental relative humidity), and can be described by

$$\rho = \rho_0 \left(\frac{t}{t_0} \right)^m k_{\text{RH}} k_{\text{T}} \quad \text{with} \quad t \le 1\,\text{year} \tag{1.20}$$

where ρ_0 is the concrete resistivity measured at age t_0, the exponent m is the aging exponent related to the electrical resistivity, k_{RH} is the influence factor of relative humidity on the resistivity, and k_{T} is the influence factor of temperature. This expression is adapted from the DuraCrete model on corrosion rate. The original model also included the influence factors of curing condition and the chloride concentration. According to Yu *et al.* (2014), the factor k_{RH} can take the following form:

$$k_{\text{RH}} = \left(-1.344h^2 + 3.709h - 1.365 \right)^{-1} \quad \text{for} \quad 50\% \le h \le 100\% \tag{1.21}$$

The factor k_{T} takes the following form:

$$k_{\text{T}} = \frac{1}{1 + \alpha_{\text{T}}(\theta - \theta_0)} \tag{1.22}$$

with α_{T} (°C^{-1}) a coefficient and θ and θ_0 (°C) the ambient and reference temperatures. Further, as the corrosion is assumed to reduce the cross-section of steel bars uniformly, the corrosion rate (units of mm/a or μm/a) can be estimated through Faraday's law as

$$\dot{r} = 0.0116 I_{\text{corr}} \tag{1.23}$$

with $\dot{r}$ (mm/a) the corrosion rate and I_{corr} (μA/cm^2) the corrosion current density.

The combined model from Equations 1.19 to 1.23 describes the resistance-controlled corrosion of reinforcement steels and considers the concrete compactness through the electrical resistance. The influence of the humidity and temperature is included in the concrete resistivity, and the time dependence of resistivity is also included to take into account the microstructure evolution of concrete during the service life. This model can be extended without difficulty to include other factors, such as initial chloride content in concrete. Since all parameters are macroscopic the model can be easily used in applications. However, several drawbacks are to be noted for this model. First, the measurement and quantification of corrosion current are subject to significant dispersion and dependent on the test methods, and no dispersion analysis for this model is available. Thus, for a practical case the credibility of model should go to the predicted magnitude than the predicted value. Second, the model considers only the resistance-controlled mechanism; thus, the valid humidity range of this model is below 90%, and the model gives a conservative estimation for the higher humidity range. Finally, the model, from Equations 1.19 to 1.22, was calibrated mostly from short-term tests in the laboratory, and so the validation of long-term in-situ tests is needed.

Nevertheless, this model of corrosion current includes the main mechanism of carbonation-induced corrosion and the main influential factors, and the prediction on corrosion rate can be helpful for engineering application. Figure 1.13 shows the simulation results for the corrosion current in terms of concrete cover, relative humidity, and concrete resistivity. The relevant parameters and their usual value ranges are given in Table 1.3. Note that a corrosion current of less than 0.1 μA/cm^2 is commonly regarded as the passivated state for steel.

1.4 Basis for Design

1.4.1 Structural Consequence

The corrosion products, identified as a compound of $Fe(OH)_2$ and $Fe(OH)_3$ (Liu and Weyers, 1998), have an expansive nature. With the formation of the products, a local stress can accumulate on the interface between the concrete and steel that is high enough to facture the concrete cover. As the corrosion develops further, the corrosion products can augment the width of the surface cracks until spalling of the concrete cover occurs. Meanwhile, the adhesion between the concrete and steel can be destroyed by the corrosion products, and the bonding strength of the concrete–steel interface is reduced. The direct consequence of this bond loss is the reduction of the RC element stiffness, particularly for RC beams in bending. The aforementioned issues constitute the main concerns for corroded RC elements for the service limit state (SLS); that is, the fracture of the concrete cover, the spalling of the concrete cover due to crack width augmentation, and the reduced element stiffness due to bond loss of concrete–steel interface.[3] The corrosion rate in Equation 1.23 was used as a basic indicator to quantify the impact of corrosion on RC elements. The following model was given for the fracture limit for a corroding steel bar (DuraCrete, 2000):

$$\Delta r_{\mathrm{f}} = a_1 + a_2 \frac{x_{\mathrm{d}}}{\phi_{\mathrm{d}}} + a_3 f_{\mathrm{t,sp}} \tag{1.24}$$

where Δr_{f} (mm) is the corrosion depth of steel bar needed to fracture the concrete cover, a_x ($x = 1,2,3$) are model parameters (74.4 μm, 7.3 μm, and −17.4 μm/MPa respectively), x_{d} and ϕ_{d} are respectively the concrete cover thickness and the diameter of the steel bars, and $f_{\mathrm{t,sp}}$ (MPa) is the splitting tensile strength of concrete. From this expression, normally a corrosion

---

[3] It is observed from experiments that a slight extent of steel corrosion, up to 4% in mass loss, can help to augment the bond strength (Li C.Q. *et al*., 2014c). However, this observation should be treated with caution since a general and uniform corrosion extent is always assumed in these studies. In real cases, corrosion, even induced by carbonation, can present nonuniform characteristics, and this threshold can lose its sense.

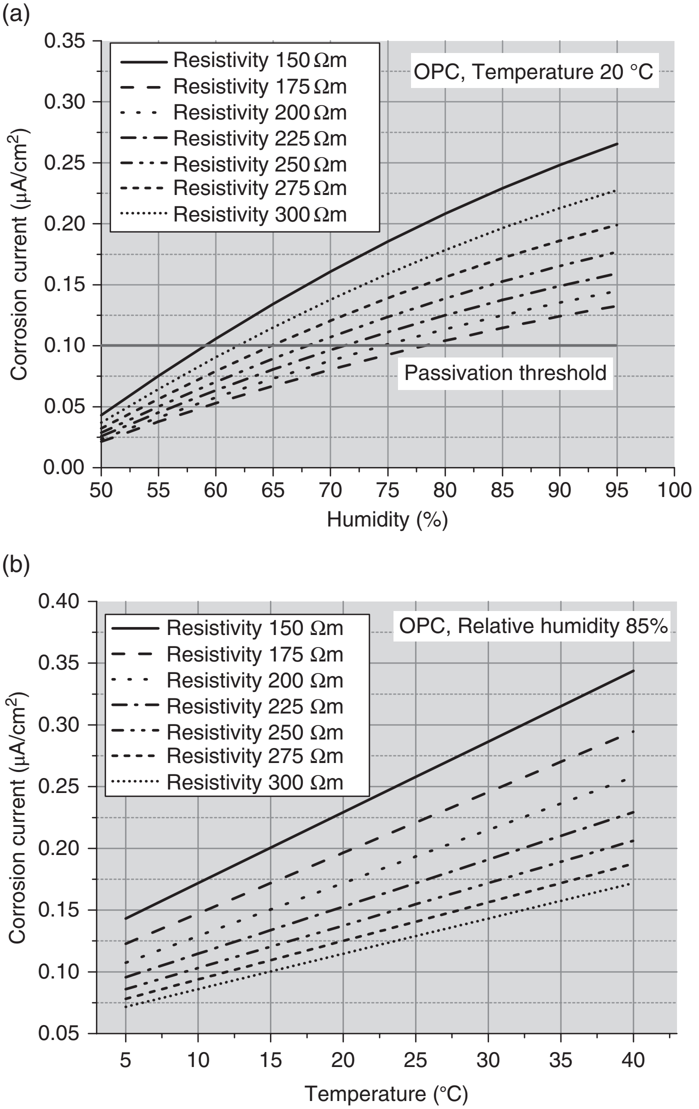

Figure 1.13 Simulation results from model C-4 for corrosion current in terms of relative humidity (a) and ambient temperature (b). The local resistivity data are retained for OPC concrete: resistivity measured at 28 days ranges from 150 to 300 Ω m for a *w*/*c* ratio from 0.6 to 0.3.

depth of 50—100 µm corresponds to the fracture limit state of the concrete cover. The following expression was proposed to account for the augmentation of surface crack width with the corrosion depth into steel bars (DuraCrete, 2000):

$$w_c = 0.05 + b_{crack}\left(\Delta r - \Delta r_f\right) \tag{1.25}$$

Table 1.3 Model parameters for the C-4 model and their usual value ranges

Parameter (unit)	Value/relation
Reference potential gradient V_0 (V/m)	0.76
Ageing exponent of electrical resistivity m	0.23 (OPC), 0.54 (GGBS), 0.62 (PFA)
Reference time t_0 (year)	0.0767 (28 days)
Resistivity of concrete measured at t_0, ρ_0 (Ω m)	150–300 (OPC), 250–550 (GGBS), 350–500 (PFA) ($w/c = 0.3 - 0.6$)
Humidity influence factor k_{RH}	1.0 ($h = 100\%$) to 6.52 ($h = 50\%$)
Environmental humidity h (%)	50–95
Temperature factor coefficient α_T (°C^{-1})	0.073 ($\theta > 20$°C), 0.025 ($\theta < 20$°C)
Reference temperature θ_0 (°C)	20.0

PFA: pulverized-fuel ash.

where w_c (mm) is the crack width and the parameter b_{crack} is equal to 0.1 and 0.125 for top cast and bottom cast bars respectively. Taking the conventional crack control width for an RC element in design, this expression gives a corrosion depth of 25 μm from cover fracture to crack width attaining 0.3 mm, which is a rather short delay. Accordingly, from a design point of view, these two stages can be conservatively combined into one state, taking Δr equal to 50–100 μm as the criterion.

As the corrosion develops further, the loading capacity of RC elements can be affected through different aspects of deterioration: the spalling of the concrete cover between corrosion cracks, the reduction in cross-section of the steel bars, the reduced ductility and tensile strength of the steel bars, and the loss of bond strength of the steel bars in the concrete section. The spalling of the concrete cover reduces the concrete section and exposes the steels more directly to aggressive environments; the reduced section of steel bars deceases directly the loading capacity of the RC section, while the reduced ductility of steel bars will decrease the resistance capacity of RC elements to dynamic loadings. The loss of bond strength reduces the loading capacity of the RC section mainly through the decrease in the effective area in compression. It was shown that the reduction of bonding strength can be as much as 90% as the bar section loses 20% of its mass (Li C.Q. *et al.*, 2014), and the flexural deflection of corroded RC beams is mainly due to the bond loss (Castel *et al.*, 2011). On the basis of the available knowledge, some standard assessment methods were proposed for loading capacity for the column and beam sections; see DuraCrete (1998). Since the corrosion extent is never allowed to develop further than affecting the SLS, the quantitative aspect of structural performance of RC elements in the post-corrosion phase is not elaborated in this text.

1.4.2 Design Considerations

The durability design is to be presented in a systematic way in Chapter 7, but some aspects specific to carbonation-induced corrosion are discussed here. The durability design of RC elements against carbonation-induced corrosion should be performed at both the materials level and the structural level for a given intensity of environmental action and expected design working life. At the materials level, the compactness of concrete materials can always help because with high compactness concrete has higher resistance to CO_2 diffusion and a higher electrical resistance to control effectively the corrosion current in the normal humidity range. To resist carbonation and provide a highly alkaline environment for reinforcement steel, a high CH content in concrete in its hardened state is appreciated in durability design; that is, OPC is favored as a concrete binder. However, some kind of compromise can be made between the compactness of concrete achieved and its CH content: with the extensive practice of incorporating SCM in concrete binders, the CH can be consumed by the secondary hydration of the mineral SCM but a high compactness can also be achieved as a result. According to state-of-the-art knowledge, high compactness seems to be favored over the CH content; that is, as long as the compactness is achieved the CH content is no longer a concern. On the last point, extensive cracks at an early age should be avoided to assure the compactness of the concrete.

At the structural level, the concrete cover thickness should be adequate to provide sufficient resistance to CO_2 diffusion. Since RC elements can bear working cracks with a certain opening width at the concrete surface, these openings are believed to accelerate CO_2 diffusion as well as the subsequent corrosion process. Normally, the cracks with opening width below 0.3 mm are regarded as harmless for carbonation-induced corrosion (Li K.F. *et al.*, 2014b). According to state-of-the-art concrete technology and experiences, high compactness of concrete, adequate cover thickness, and efficient control of working cracks can provide RC elements and structures with service lives of 50 years or longer without additional protection measures. As RC elements and structures are subject to other environments, carbonation is always the fundamental process for other deterioration processes. In this case, the possible intervention of carbonation in other deterioration processes should be treated in the design.